Supporting Information

Usoskin et al. 10.1073/pnas.0914705107

SI Materials and Methods

Chamber Preparation and Cell Culturing. A 14-mm hole was drilled in the center of a regular 35-mm cell culture plate (BD Biosciences). A 25-mm circular glass coverslip coated with poly-D-lysin was fixed by silicone grease (Corning) to cover this cavity. Chambers were mounted from parts cut out of Thermanox plastic coverslips (Nunc). Double-sided sticky gasket (Emsdiasum) was used to attach the "pillars" to the coverslip (Fig. S1 *A* and *C*). Bridges were attached to the top of these pillars by BF-6 glue (Verteks Ltd.). Thus, the two bridges separated three compartments (Fig. S1 *A* and *C*): two outer and one central. To guide directional axon growth, cells were cultured with a growth-factor gradient whose formation was facilitated by providing a growth factor-rich cell-culture medium in one of the outer chambers (referred to as a "+" chamber). The bridge, separating the central chamber from the "+"chamber was termed the "+" bridge. Media lacking growth factors was added to the opposite outer chamber and, therefore, this chamber and its bridge were designated as the "–" bridge. A hydrophobic pen was used to mark the whole cover slide and the top of the bridges to prevent the leakage of neurotrophic factor (NF)-containing media.

A mixture of four NFs was used: NGF (R&D Systems), NT-3 (Promega), BDNF (Promega), and glial cell line-derived neurotrophic factor (R&D Systems). When preparing dissociated neuron cultures, matrigel [95%, (MG); BD Biosciences] was allowed to seal the space under the bridge by way of surface tension. MG/NF mixture (20 ng/mL each) was used to load the "+" bridge, whereas pure MG was applied to the "–" bridge. MG was allowed to solidify in a CO_2 incubator within 3 to 5 min. Subsequently, the central chamber was coated by laminin (30 μg/ml; Cultex mouse laminin, R&D Systems; 2 to 4 h at 4 °C). Sensory neurons were isolated according to published protocols (1). Cells were plated at 90% confluence in DMEM/F12 supplemented with N2 and 10% fetal calf serum. The medium in the central chamber was replaced with DMEM/F12, supplemented with N2 (Gibco), 2% B27 (Gibco), gentamicin, and NFs (1 ng/mL each) 2 h after plating. Media were replaced in every compartment every other day. Mechanical stimuli were applied to the "+" bridge (Fig. S1 *A*, *C*, and *D‴*).

Stimulation Setup. A piezo bender (Physik Instrumente GmbH) was used to provide mechanical stimulation. This bender is equipped with an integrated piezo sensor that monitors the bender current position. A small clip carrying an iron pin (probe) was attached to the tip of the bender (Fig. S1*E*). Probes were calibrated under the microscope. The bender was controlled by driving voltage applied by a computer-controlled system run in an open feedback loop: that is, the voltage applied to the piezo controller was transmitted into the driving voltage of the bender. This process allowed for accurate probe positioning above the bridge. We estimated the probe's positioning accuracy to be within 1.6 μm. A computer program was developed to control the stimulation device, perfusion valve controller, and data acquisition and integration (i.e., exact time, duration, and strength of mechanical or chemical stimulation in synchrony with Ca^{2+} imaging).

Magnitude of Mechanical Stimuli. In a series of calibration experiments, we identified the maximum amplitude of static indentation (80 μm), which neither disintegrated the axons nor detached them from the slide surface. Therefore, we have applied static indentation up to 60 to 70 μm in a routine experiment. Maximal vibration magnitudes were 40 to 50 μm, because we reasoned that vibration stimuli would be more destructive to the gel and axons. Furthermore, saturated vibration responses were often observed at 30- to 40-μm vibration amplitudes. Thus, the maximal amplitude of vibration stimuli was generally 10 to 20 μm smaller than that used for static indentation. Trains of successive stimuli were programmed, including both static indentation (from 20 to 70 μm indentation, ramp 900 mm/s, duration 5–10 s) and vibration (different magnitude of displacement, frequency, and duration, as indicated).

Probe Positioning. The probe was first visually positioned above the center of the "+" bridge. Subsequently, the probe was slowly lowered while monitoring the sensor voltage (through the embedded piezo sensor monitoring the actual bender position). As soon as the probe came into contact with the bridge, their simultaneous initial bend was reflected by a change in the bender's sensor voltage. According to the manufacturer's specification, 1 mV of sensor voltage corresponds to 40 nm of bender tip displacement, with the bender's stiffness specified at 10 mN/μm. As soon as a 1- to 2-mV change of sensor voltage was observed, the bender was slightly retracted. Using a calibrated Von Frey hair filament and by observing plastic bridge bending under microscope, we estimated the stiffness of the bridge to be about 0.5 mN/μm. We approximate that when the sensor's voltage change is noticeable (1–2 mV), the bender itself has already bent up to 80 nm. This theory corresponds to ≈1.6 μm of bridge bending. Thus, when the probe was positioned, the bridged was temporarily bent to 1.6 μm (note the thickness of the MG sandwich being ~270 μm), which we have considered as an inherent and negligible probe positioning error, given the range of mechanical stimulation ranging from 20 to 70 μm.

Provided that the "bridge" is significantly wider than the area from which we have recorded, we estimated that a variation in the displacement of the bridge along the stretch of the recorded area could not exceed 1% (see below), which should not affect the results we obtained.

Distance from the Soma to the Stimulating Bridge Does Not Correlate with Sensitivity or Response Profile. The geometry of the chamber invariably results in recorded cells being situated at varying distances from the bridge. To confirm that this does not affect cellular responses, we correlated the distance of a static neuron from the bridge with the minimum bridge indentation required to evoke a threshold somatic Ca^{2+} response ($\Delta R/R_o$ threshold = 0.2). We found no correlation (Fig. S2*A*), suggesting that the static neurons' sensitivity to mechanical stimuli is not dependent on their somatic distance to the bridge. In fact, none of the mechanosensitive subtypes described below showed any correlation between their response characteristics and their location in the chamber.

Estimation of Pressure Differences on Axons at Different Positions Along the Bridge. Axons grow under the bridge grossly parallel to each other and perpendicular to the bridge (Fig. S1*B*). Because we always captured Ca^{2+} responses from neurons situated within 0.5×0.5 mm^2 adjacent to the centrum of the spring (Fig. S1*D‴*, yellow square), we reasoned that their axons situated also within the ±0.25-mm area along the central axis of the bridge. With this assumption, we estimated (Fig. S5) that difference in the thickness of the gel after compression (which presumably correlates to local pressure experienced by axons) above the middle of the bent bridge and 0.25 mm beside it does not exceed 1%. Such a difference should be considered as negligible.

Fine Aspects of Mechanical Stimulation. Our first attempts to record receptor currents (RCs) using conventional design plates failed because of the recorded cells being situated too close to the stimulus source (the bridge). At such distance, stimulation resulted in gel squeezed out from under the bridge and pressing onto the cells' somata. Recording in such conditions did not allow us to distinguish signals generated at axons from those produced by somatic stimulation. To address this issue, we introduced stretched capron fibers above and perpendicular to the proximal part of axons (Fig. S3). This modification reduced the threshold of mechanical stimuli, minimizing the gel displacement from under the bridge and allowing for artifact-free recordings from neurons proximal to the bridge. To ensure that the generated currents resulted from the stimulation on axons, and not the soma, several cells ($n = 5$) situated at the same distance from the capron fiber were recorded. Among these cells, some responded to stimulation with action potentials (APs). Among the proximal responders, not all exhibited RCs when recorded during stimulation, presumably because of longer axonal distances from the site of RC generation and to subsequent signal attenuation below acceptable signal-to-noise levels. Overall, our results help excluding the involvement of somatic mechanosensitive channel activation.

Mechanical stimuli applied to the bridge of conventional design chambers (i.e., without fibers) can result into two types of mechanical disturbances of axons: vertical compression and, possibly, longitudinal stretching. The specific effects of each on stimulation response (both in our system and in vivo) are difficult to distinguish. The presence of fibers with constant amplitude of stimulation should increase the probability of a more focal compression without significant stretching. Because the introduction of capron fibers reduces the stimulus amplitude required to evoke reliable responses by 2- to 3-fold, the recorded neuronal response under such design is much more likely to be elicited by local focal compression stimuli. Interestingly, when being activated at lower stimulation amplitudes, the response profiles observed in plates with and without capron fibers were comparable, indicating that modes of mechanical activation of channels are similar in both cases.

Similar mechanosensitive channels can potentially exhibit different responses when activated in neuronal somata, which is largely spherical in shape, and in axons. Theoretically, differences could be caused by both extracellular matrix components and the cytoskeleton, both of which are implicated in mechanoreception (2, 3). One indication for this effect is the fact that many mechanical-sensitive units in vivo fire APs during the release phase of static indentation (4). However, corresponding RCs have not been recorded in studies where soma was stimulated by poking. In our system, we often recorded APs at the release phase of static indentation (Fig. 1*E*), similar to those reported ex vivo.

Increasing focal compression by introducing capron fibers also allowed us to address the question of distribution of mechanically gated channels along the axons. Plates where fibers were situated on top of proximal versus distal parts of axons demonstrated similar sensitivity profiles. This observation suggests that mechanosensitive channels are expressed along the whole length of axons and not at any specific segment, which is the case in a neuropathic/inflammatory pain model but not in a normal situation in vivo.

1. Hjerling-Leffler J, Alqatari M, Ernfors P, Koltzenburg M (2007) Emergence of functional sensory subtypes as defined by transient receptor potential channel expression. *J Neurosci* 27:2435–2443.
2. Wetzel C, et al. (2007) A stomatin-domain protein essential for touch sensation in the mouse. *Nature* 445:206–209.
3. Hu J, Chiang LY, Koch M, Lewin GR (2010) Evidence for a protein tether involved in somatic touch. *EMBO J* 29:855–867.
4. Koltzenburg M, Stucky CL, Lewin GR (1997) Receptive properties of mouse sensory neurons innervating hairy skin. *J Neurophysiol* 78:1841–1850.

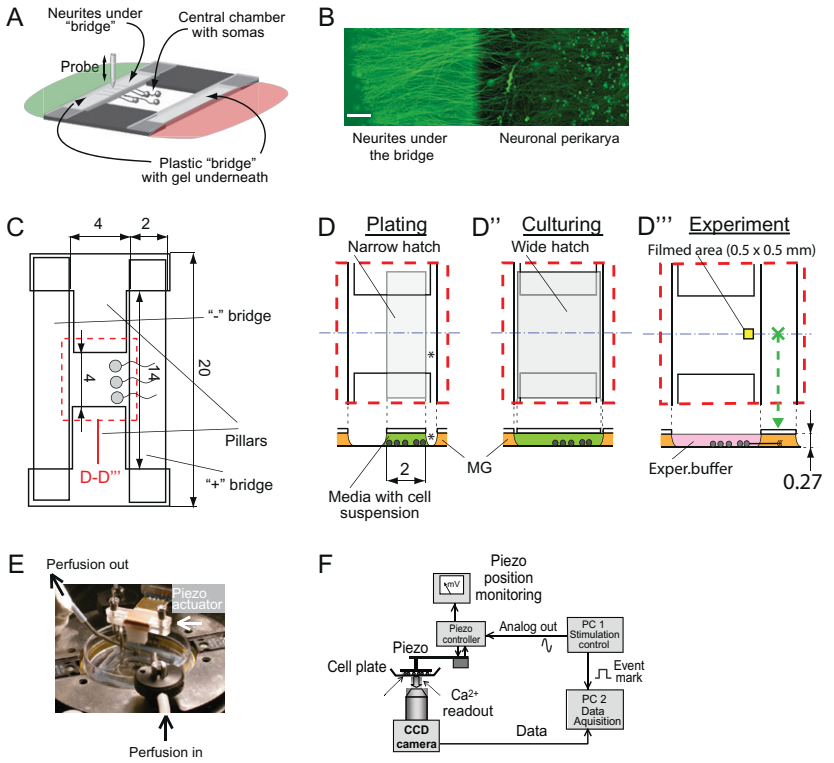

Fig. S1. (*A*) Schematic design of the recording chamber. (*B*) Neurite ingrowth under the bridge after 5 d in vitro as revealed by β-III-tubulin immunoreactivity of neuronal processes. (Scale bar, 150 μm.) (*C*, *D*, *D″*) Schematic drawing of the "bridge-over-gel" chamber with sizes specified (*C*), and setup during seeding (*D*), culturing (*D′*), and recording from cells (*D‴*). All distances are in millimeters. Sensory neurons are depicted in the central compartment sending axons under the "+" bridge. (*D–D‴*) Central compartment of the bridge-over-gel chamber (indicated in *C* by a red rectangle). (*Upper*) Views of the chamber from above and (*Lower*) side view cross-sections through the middle of the central compartment (as indicated by the horizontal dashed blue line in the top drawings). (*D*) Various experiments aimed to optimize directional neurite growth demonstrated the pivotal role of the bridge-over-gel chamber design during cell seeding. A clear border between densely seeded neurons and an area free of cells between neuronal somata and the spring improves directional neurite growth. To generate such a border region, we have allowed a dense cell suspension containing dissociated neurons to be sucked by surface tension under a narrow hatch made of thin plastic. Because underneath the edges of this hatch the solution edge was close to vertical, such configuration allowed for an even and dense attachment of the cells under the hatch and resulted in a well-defined border. Immediately after cell-seeding, the hatch was slid as close as possible to the "+" bridge, but with negative meniscus (*) separating cell suspension from the MG. Two hours after seeding, the plating media (DMEM/F12 supplemented with N2 and 10% FCS) was replaced by 1 ng/mL NGF in DMEM/F12 supplemented with N2 and B27. This procedure was performed without removing either the hatch or the entire preceding medium. Instead, excess replacement media was added to form a large meniscus, resulting in the hatch floating on top because of surface tension. Subsequently, we have aspirated the medium until the hatch sat onto the pillars. This procedure was performed twice. Neurotrophin-containing media was applied to the "+" compartment. In contrast, neurotrophin-free media was added to the "−" compartment. (*D′*) On day 2, media were refreshed in all compartments. The narrow hatch covering the central chamber was replaced with a wide hatch that has covered the entire width of the central chamber. This configuration minimized disturbance to the neurotrophin gradient that had been established overnight and provided a local environment facilitating axonal growth. (*D‴*) Prior to recording, we removed the hatch covering the central chamber. The yellow square indicates the position of the field of recording (proportional in size to that of the central chamber). Position of the probe pressing onto the bridge is indicated (X) with its projection in the side view being depicted by a dashed arrow (—); 0.27 indicates thickness of the gel. (*E*) View of a plate with the chamber in the experimental setup. (*F*) Scheme of automated experimental setup for studying mechanosensation in sensory neurons. Electrophysiological recording setup is not included.

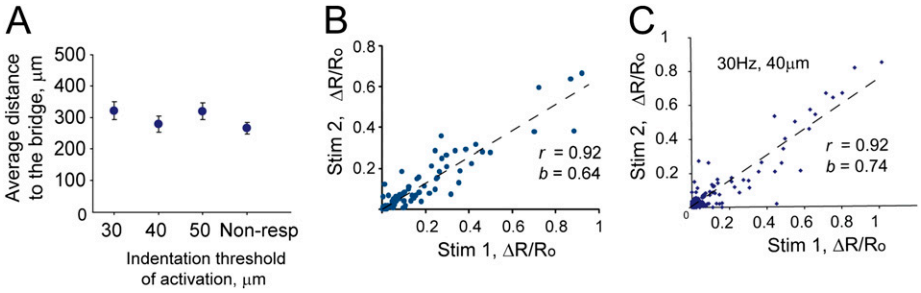

Fig. S2. (*A*) Sensitivity to static stimulation does not depend on the distance of neuronal somata from the spring. Static responding neurons were grouped based on the minimal threshold of indentation stimuli to which a response in $[Ca^{2+}]$ ($\Delta R/R_o$) exceeded a threshold of 0.2. Mean distance of somata from the bridge was calculated for each group (n = 153, N = 1). (*B* and *C*) Cellular responses to two consecutive indentation (*B*) or vibration (*C*) stimuli demonstrate the reproducibility of response patterns. Correlation coefficient (r) and regression line slope (b) have been specified.

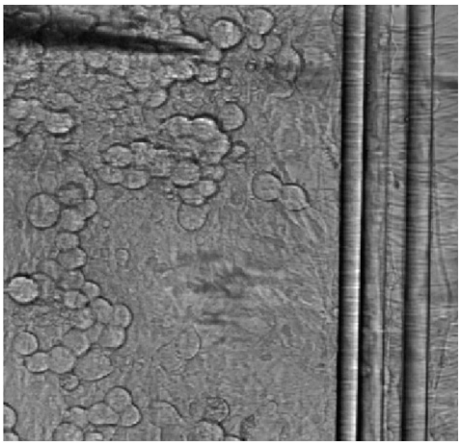

Fig. S3. Capron fibers (three pieces) stretched above axons grown under MG. Such configuration reduced bridge displacement required to trigger mechanical responses in neurons by 2- to 3-fold and permitted recording of RCs. Patch pipette can be seen in the upper left corner.

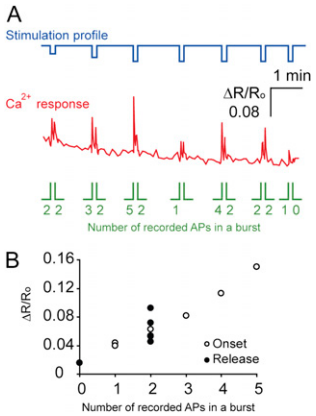

Fig. S4. Correlation between the Ca^{2+} amplitude and the number of APs triggered by onset or release of static indentation stimuli. (*A*) Simultaneous Ca^{2+} imaging and electrophysiological recordings of APs in response to seven consecutive static stimuli (blue). Ca^{2+} trace is shown in red. The number of APs recorded is depicted in green. (*B*) The number of APs plotted against the amplitude of the Ca^{2+} response. These data suggest that the relatively low acquisition rate (1 Hz) of Ca^{2+} transient monitoring does not compromise the sensitivity of our method and allows the registration of single APs at neuronal somata.

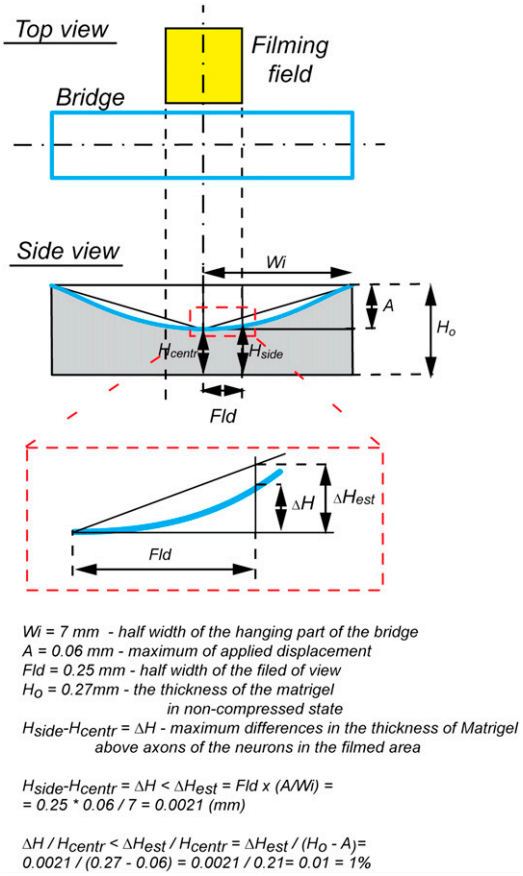

Wi = 7 mm - half width of the hanging part of the bridge
A = 0.06 mm - maximum of applied displacement
Fld = 0.25 mm - half width of the filed of view
H_O = 0.27mm - the thickness of the matrigel in non-compressed state
H_{side}-H_{centr} = ΔH - maximum differences in the thickness of Matrigel above axons of the neurons in the filmed area

H_{side}-H_{centr} = ΔH < ΔH_{est} = Fld x (A/Wi) =
*= 0.25 * 0.06 / 7 = 0.0021 (mm)*

ΔH / H_{centr} < ΔH_{est} / H_{centr} = ΔH_{est} / (H_O - A)=
0.0021 / (0.27 - 0.06) = 0.0021 / 0.21= 0.01 = 1%

Fig. S5. Difference in the compression of the gel above the imaging field neurons' axons does not exceed 1%. (*Top*) Top view of the bridge span (blue contour) with adjacent imaging field (yellow square). (*Middle*) Side view of the bent bridge (blue curve) with compressed gel underneath (gray). Because axons mainly grow parallel to each other as well as perpendicular to the bridge, axons from neurons that are situated within the field of view should be located under the middle area of the bridge. (*Bottom*) Enlargement of the outlined area in the *Middle*, with size specifications and calculations demonstrating that bridge displacement differences (ΔH/H) above projection of filming view to the bridge does not exceed 1%.